Theory Analysis and CFD Simulation of the Pressure Wave Generator

Bing Yang, Jianqiang Deng*, Kai Liu, Fanghua Ye

School of Chemical Engineering and Technology, Xi'an Jiaotong University, Xi'an, Shaanxi 710049, China
dengjq@mail.xjtu.edu.cn

In a pressure wave generator mainly consisting of a stator and a rotor with several valve blocks, pressure waves are generated by the continuous shear perturbation of fluids. In this paper, theory analysis of pressure wave generated in water hammer principle was conducted. Then a simplified CFD model of a pressure wave generator connecting the upstream and downstream pipes was established, and the grid and the time step independence tests were carried out. Generating process of controllable pressure waves in pipe flows was simulated, and the frequency and amplitude characteristics were obtained. The results suggest that pressure waves in upstream and downstream pipes have the similar shapes of approximate sinusoidal waveform and opposite phase. Pressure is inversely proportional to the first order derivative of x-velocity at a certain position, which is in good agreement with theoretical analysis; pressure wave amplitude increases with an increment of the rotational frequency of the rotor at the beginning of the pressure wave generator operation, but reaches the maximum amplitude in an optimal frequency when the generator is in stable operation, which means there exists a transition process for the generator. The critical frequency related to the first characteristics time can be applied to avoid the waveform distortion.

1. Introduction

Pressure waves in transient flow are generally induced by flow disturbances which may be caused by planned or accidental changes in a system (Chaudhry, 2014). Pressure waves with high propagation speed and energy concentration properties can be utilized in transmission signal in measurement while drilling system during drilling process (Patton et al., 1977). Another significant application of the pressure waves is the early detection of gas influxes because of encountering gas-bearing fractures in gas drilling process to prevent the accidents and ensure security and continuity of gas drilling (Meng et al., 2015). Pipe leakage may cause wastes for water and energy resources and can produce contaminants in urban water supply systems. Pressure waves can also be applied in identifying and detecting potential defects in water supply pipe systems (Duan, 2017).

Fang and Su (2004) summarized the fundamental types of the pressure wave generator in a measurement while drilling system in petroleum drilling engineering, and classified pressure wave generators into two main categories including the depressurization type and throttle type. The principle of the pressure wave generator based on the thin-walled cutting edge flow characteristics was analyzed and the curve orifice generating the continuous sinusoidal pressure wave was designed and optimized (Jia et al., 2010). Xue et al. (2011) designed a new type pressure wave generator applied in vibration cementing based on water hammer theory. In order to obtain an optimized valve orifice satisfying the requirements for the continuous sinusoidal pressure output, an improved arc-fillet-line triangular valve orifice was designed based on a general line triangular valve orifice (Yan et al., 2015). Hansen and Kjellander (2016) employed the CFD method to explore the consequences of a sudden opening of a storage tank due to an external aggression and analyzed characteristics and attributions of the pressure waves.

Although many studies have been published concerning the applications of the pressure wave and generator and qualitative analysis of pressure wave characteristics, a little of research has been done on generating controllable pressure wave and theory analysis of pressure wave generator are inconsistent in different literatures. In the present paper, theoretical analysis is carried out by extending classic water hammer theory

in continuous transient process and CFD simulations of pressure wave generated in the generator are conducted. The simulation results reveal the amplitude and frequency characteristics which are discussed quantitatively.

2. Mechanism of a pressure wave generator

2.1 Theory analysis

Water hammer with spatial and temporal changes in velocity and pressure in pipe systems is caused by rapid flow disturbances; such transient flows are assumed to be unidirectional because the axial fluxes of mass, momentum and energy are far greater than their radial counterparts (Ghidaoui et al., 2005).

With the unidirectional assumption, the one-dimensional water hammer governing equations in transient pipe flows can be derived by applying the principles of mass and momentum conservation to a control volume in an oblique tapered pipe. The continuity equation for a control volume is expressed as follows:

$$V\frac{\partial P}{\partial x}+\frac{\partial P}{\partial t}+\rho c^2\frac{\partial V}{\partial x}-V\sin\alpha=0 \tag{1}$$

where v is the x-direction velocity, P is the pressure, α is the angle between pipe centreline and the horizontal line, g is the gravitational acceleration, c is the wave speed, ρ is the density of fluid. Considering gravitational, wall shear and pressure gradient forces as externally imposed, the momentum equation can be given by:

$$\frac{1}{\rho}\frac{\partial P}{\partial x}+V\frac{\partial V}{\partial x}+\frac{\partial V}{\partial t}+\frac{fV|V|}{2D}=0 \tag{2}$$

where D is the inner diameters of the pipe, f is the friction coefficient. The wave speed can be calculated by:

$$c^2=\frac{K/\rho}{1+\left[(K/E)(D/e)\right]c_1} \tag{3}$$

where K is the bulk modulus of elasticity of the fluid, E is the Young's modulus of elasticity of pipe materials, e is the thickness of the pipe, c_1 is the parameters related to the constraint conditions of the pipes. Eq(1-2) can be used in 1D compressible pipe flow.

Compared to other terms in Eq(1-2), the convective terms are negligible in magnitude because the wave speed is considerably larger than x-direction velocity of fluid in most of the engineering applications (Chaudhry, 2014). To analyze the pressure wave propagation characteristics, the fluid is supposed to be inviscid. Based on the above assumptions and simplifying the equations, the pressure wave equation can be written as:

$$\frac{\partial^2 P}{\partial t^2}=c^2\frac{\partial^2 P}{\partial x^2} \tag{4}$$

which is a one-dimensional second-order wave equation.

For the case of a rapid closure of the downstream valve in a piping system with a constant level reservoir at the upstream end and a valve at the downstream end, the general solution of Eq(4) is represented as:

$$\Delta P=\rho c\Delta v \tag{5}$$

It can be noticed from Eq(5) that the pressure wave amplitude is proportional to change in x-direction velocity. The disturbance of the case for the rapid closure of the valve is instantaneous and discontinuous. For a continuous disturbance case, the process can be viewed as a linear superposition of instantaneous closure process at each moment. Assuming that ρ and c are constant, the partial derivative of time on right side of Eq(5) can be calculated to obtain the relationship between the pressure and the x-direction velocity which can be written as:

$$\Delta P(t)=k\rho c\cdot v'(t) \tag{6}$$

where k is the correction coefficient. The Eq(6) can describe the quantitative relation between the pressure and the velocity accurately, which may validate the simulation results in Part 4.

2.2 Construction and working principle

A pressure wave generator shown in Figure 1(a) mainly consists of a stator, a rotor, a shaft, an upstream pipeline and a downstream pipeline. Both the stator and rotor are fan-shaped and have four valve blocks. When the generator works, the stator remains stable and the rotor driven by a variable frequency motor rotates at a certain speed to disturb the fluid flow in both upstream and downstream pipes continuously. As mentioned for continuous disturbances, variation in pressure is closely related to change rate of velocity.

Therefore, the periodic variation in velocity field which is induced by the continuous shear disturbance will produce the pressure waves in the generator and waves will propagate along the pipelines.
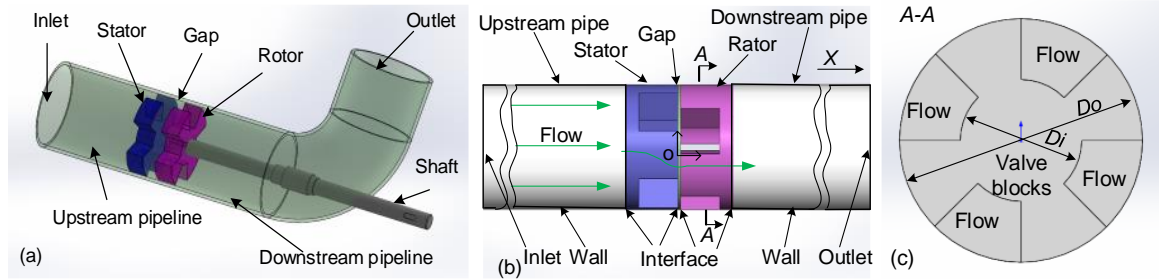
Figure 1: (a) The 3D model of a pressure wave generator, (b) The Main parts and boundary conditions of the CFD model, (c) Left view of the rotor

3. CFD method

3.1 CFD modelling

In order to investigate the generating process and characteristics of pressure waves, the effect of the bend pipe on pressure wave is neglected and the pressure wave generator system can be reduced to five parts, including an upstream pipe (length: L_u = 5,000 mm, diameter: D_u = 80 mm), a stator (inner diameter: D_{si} = 40 mm, outer diameter: D_{so} = 80 mm), a rotor (D_{ri} = 40 mm, D_{ro} = 80 mm), a downstream pipe (L_{d1} = 5,000 mm, D_d = 80 mm) and a gap (thickness: δ_g = 3 mm, D_g = 80 mm) between the stator and the rotor which are shown in Figure 1(b). Figure 1(c) shows the left view of the rotor to illustrate the valve block shape. The origin of coordinate system is at the centre of the left surface of the gap. Grids of each part is generated by using the ICEM CFD 14.5 and merged together. The junction surfaces of each part are defined as interface boundaries to accomplish the data communication. Attributed to the complexity of each part, the grids of the gap, the upstream and downstream pipes are structured; the stator and the rotor are meshed by tetrahedral unstructured grids. ANSYS Fluent 14.5 with 3D mode was applied to perform CFD calculations. Simulations in this paper mainly focused on the pressure wave characteristics caused by velocity fluctuations in a single phase flow and involved strong unsteadiness occurring in the flow. The realizable k–ε turbulence model was chosen to simulate the pressure wave better (Yang et al., 2015). The motion of the rotor was achieved by setting in the cell zone motion dialog box. All types of boundary conditions and corresponding values are presented in Table 1. Considering slight compressibility of water as the fluid in cases, the density of water was determined by a user defined function(UDF) of pressure (ANSYS., 2012). The density of water was calculated by the following equation:

$$\rho = \rho_{ref} \Big/ \left(1 - \left(P - P_{op} \right) \big/ K \right) \tag{7}$$

Where ρ_{ref} is the reference density, ρ_{ref} = 998.2 kg/m³; P_{op} is the operating pressure, P_{op} = 101,325 Pa; K is the bulk modulus of elasticity of the fluid, K = 2,180 MPa. All the details regarding the chosen solver settings are given in Table 2. In all cases, the steady results remaining the rotor stationary were obtained to be the initial conditions for unsteady calculations. Monitoring surfaces along the axis positioned by the different x-coordinates were created to achieve the pressure and velocity at certain positions, which were named by the x-coordinate and the measurement units in m.

Table 1: Boundary conditions

Part of geometry	Inlet	All walls	All interfaces	Outlet
Boundary condition type	Pressure inlet	Stationary wall, no slip	Interface	Pressure outlet
Value	1.005 MPa	-	-	1 MPa

Table 2: ANSYS Fluent solver settings

Solve type	Density	Wave speed	Turbulence models	Pressure-velocity coupling	Convergence criteria
Pressure-based	UDF	1,000 m/s	Realizable k–ε	SIMPLE	10^{-6} for energy 10^{-3} for the rest

3.2 Independence test

Grid independence test was performed on three meshes, consisting of the following number of nodes on per meter in axial direction of the pipe: 200 (coarse mesh), 300 (medium mesh) and 320 (fine mesh). Due to the periodic unsteady flow, time step independence test was conducted on several time steps determined by:

$$\Delta t = 1/\left(N \cdot n \cdot f_r\right) \tag{8}$$

where f_r is the rotational frequency of the rotor, N is the number of valve blocks, n is a specific integer. f_r was set to 30 Hz. Variations in x-direction velocity of the monitoring surface at x = -1 m in different mesh types and time steps are illustrated in Figure 2(a) and (b). It can be observed from Figure 2(a) that velocity variation with time between medium mesh and fine mesh is closely related. Figure 2(b) shows the velocity changes with time in different time steps cases. The medium mesh and $n = 24$ were chosen to conduct the CFD calculation.
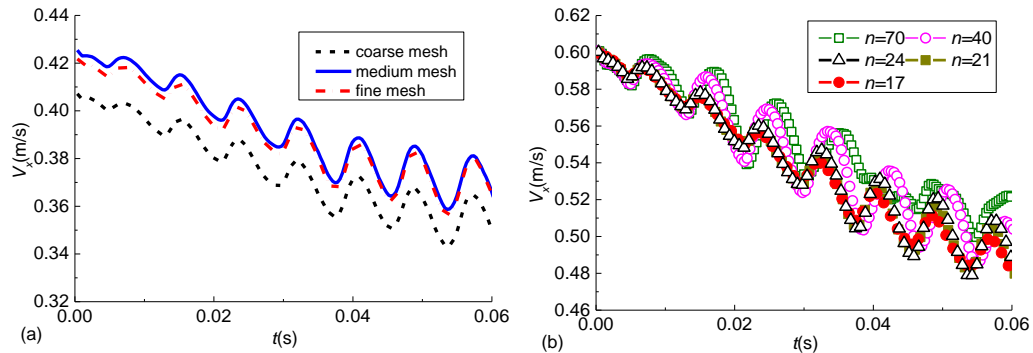
Figure 2: (a) Grid independence test, (b) Time step independence test

4. Results and discussion

Figure 3 shows the pressure variation with time in different positions at f_r = 30 Hz. Time was nondimensionalized by multiplying the frequency of the rotor and N. As shown in Figure 3, the pressure waves in upstream and downstream pipes have the similar shapes of approximate sinusoidal wave and opposite phase, which means that the compression wave in upstream and expansion wave in downstream are generated simultaneously when the rotor rotates and disturbs the flow. In different observation positions, there exists obvious phase difference because of the finite wave speed for compressible fluids.
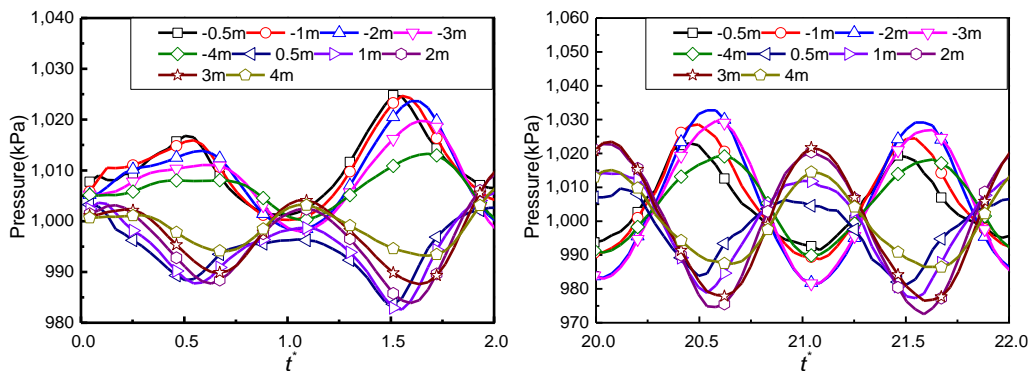
Figure 3: Pressure variation with time in different positions at f_r = 30 Hz

Figure 4(a) shows changes in the pressure and x-direction velocity of the monitoring position at x = -3 m and the opening of rotary valve with time. From Figure 4(a), it can be seen that the pressure reaches a maximum when the valve was fully closed, and reaches a minimum when the valve were totally open. In order to validate the simulation result, the first order derivative of velocity and the coefficient k in Eq(6) was calculated, and the mean value of pressure were determined. Pressure of the monitoring position at x = -3 m can be computed by using the following theoretical relation between pressure and the first order derivative of velocity:

$$P(t) = \overline{P} + k\rho c \cdot v'(t) \tag{9}$$

where $\overline{P}$ is the mean pressure at a certain position in a time series. The pressure variations of the simulation result and the theoretical calculation result with time are shown in Figure 4(b). It can be noted from Figure 4(b) that CFD results are in good agreement with theoretical results.
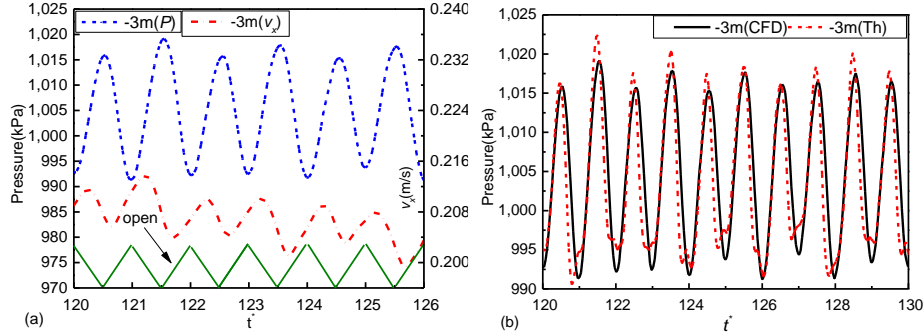
Figure 4: (a) Pressure and velocity variations with time, (b) Pressure variation of both the simulation result and the theoretical calculation result with time

Effects of the rotational frequency of the rotor on pressure waves in the pipes are shown in Figure 5(a). In Figure 5(a), it can be found that the pressure wave amplitude increased with an increment of rotational frequency at the early stage of the pressure wave generator operation. The reason for this could be that the shear disturbance of rotor to flow might increase when frequency went up in the same initial conditions. Figure 5(b) shows the frequency characteristics of pressure wave more accurately by employing the fast Fourier transform method. As shown in Figure 5(b), the amplitude of pressure increased when the rotational frequency was from 0 Hz to 30 Hz; when rotational frequency was higher than 30 Hz, the amplitude decreased as the rotational frequency went up. These phenomena may be attributed to the shear disturbance of rotor and the flow response in different rotational frequency. The waveform distortion induced by the short pipes with low rotational speed can be noticed from Figure 5(a). For a certain pipe system, there exists a critical frequency which could be estimated by the first characteristics time T_{ic} of pressure wave. T_{ic} can be computed by:

$$T_{ic} = 2L_p / c \tag{10}$$

where L_p is the length of pipe. For a given number blocks of rotor, the critical frequency can be determined by:

$$f_{cr} = 1/(N \cdot T_{ic}) \tag{11}$$

where f_{cr} is the critical frequency. To avoid the distortion, the rotational frequency should be higher than f_{cr}, which is helpful to regulate the pipe system and rotational frequency to obtain a better waveform.
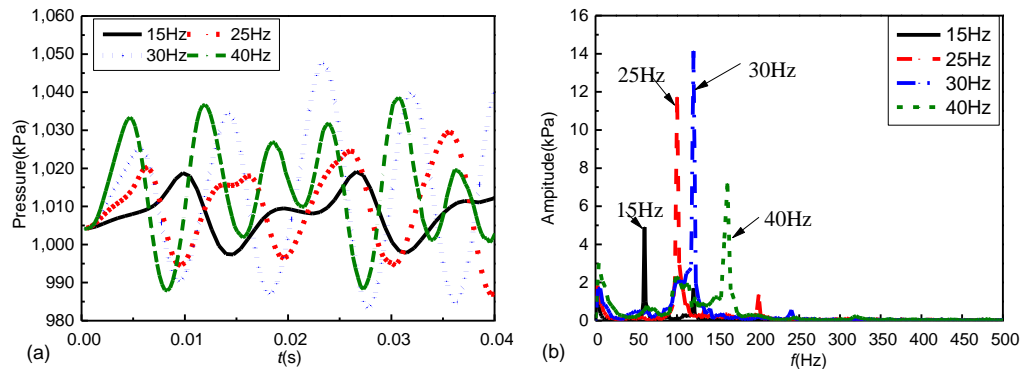
Figure5: (a) Pressure variation with time in different rotational frequency, (b) Frequency characteristics of pressure wave

5. Conclusions

In the present paper, theoretical analysis and numerical experiments on pressure wave generated in pipelines have been conducted. Extending approximate solution of water hammer theory was obtained to reveal correlation between pressure field and velocity field concisely, which may explain the generation of pressure wave in continuous disturbance flow. The simulation results were validated by theory results and showed both amplitude and frequency characteristics. Pressure wave amplitude increased with the rotational frequency at the early stage of the pressure wave generator operation but existed an optimal frequency to reach the maximum amplitude when the generator was in stable operation, indicating that there existed a transition process in the generator. And the waveform distortion will appear when the rotational frequency is lower than the critical frequency which can be avoided by regulating the pipe system and rotary frequency. Further research is needed to investigate practical operating conditions and the flow transition phenomenon in high rotational frequency. The study on pressure wave characteristics can help to apply the pressure wave in practice and achieve the velocity fluctuations in scientific research.

References

ANSYS., 2012, ANSYS FLUENT UDF Manual 14.5, ANSYS Inc, Canonsburg, PA 15317, USA.

Chaudhry M.H., 2014, Applied hydraulic transients, Springer New York, New York, USA.

Duan H.F., 2017, Transient frequency response based leak detection in water supply pipeline systems with branched and looped junctions, Journal of Hydroinformatics, 19, 17-30.

Fang J., Su Y., 2004, Fundamental types and principles of hydraulic signal generator, Petroleum Drilling Techniques, 32, 39-41.

Ghidaoui M.S., Zhao M., McInnis D.A., Axworthy D.H., 2005, A review of water hammer theory and practice, Applied Mechanics Reviews, 58, 49-76.

Hansen O.R., Kjellander M.T., 2016, CFD modelling of blast waves from BLEVEs, Chemical Engineering Transactions, 48, 199-204.

Jia P., Fang J., Li L., 2010, Design of the rotary valve of the drilling fluid continuous wave generator and analysis of the signal characteristics, China Petroleum Machinery, 38, 9-12.

Meng Y., Li H., Li G., Zhu L., Wei N., Lin N., 2015, Investigation on propagation characteristics of the pressure wave in gas flow through pipes and its application in gas drilling, Journal of Natural Gas Science and Engineering, 22, 163-171.

Patton B.J., Gravley W., Godbey J.K., Sexton J.H., Hawk D.E., Slover V.R., Harrell J.W., 1977, Development and successful testing of a continuous-wave, logging-while-drilling telemetry system, Journal of Petroleum Technology, 29, 1215-1221.

Xue L., Li B., Liu A., Zou J., Zhang W., 2011, Study of compression wave caused by hydraulic cementing tools, Petroleum Drilling Techniques, 39, 105-109.

Yan Z., Wei C., Geng Y., Shao J., Hu X., Li Y., 2015, Design of a rotary valve orifice for a continuous wave mud pulse generator, Precision Engineering, 41, 111-118.

Yang S., Chen X., Wu D., Yan P., 2015, Dynamic analysis of the pump system based on MOC–CFD coupled method, Annals of Nuclear Energy, 78, 60-69.